第29卷 第6期
2005年6月

高 能 物 理 与 核 物 理
HIGH ENERGY PHYSICS AND NUCLEAR PHYSICS

Vol.29, No.6
Jun., 2005

Response of the Neutron Star Properties to the Equation of State at Low Density *

ZHU Zhao-Huan[1] BAN Shu-Fang[1] LI Jun[1] MENG Jie[1,2,3;1)]

1 (School of Physics, Peking University, Beijing 100871, China)

2 (Institute of Theoretical Physics, Chinese Academy of Science, Beijing 100080, China)

3 (Center of Theoretical Nuclear Physics, National Laboratory of Heavy Ion Accelerator Lanzhou, Lanzhou 730000, China)

Abstract Using the RMF theory to describe the neutron liquid region in the neutron star and the Fermi gas model or FMT, BPS, and BBP model to describe the crust of the neutron star (referred as Fermi gas + RMF and RMF* respectively), the properties of the neutron star are calculated and compared with those from the RMF theory. Although the EOS at low density has negligible influence on the maximum mass of the neutron star, and its corresponding central density, energy density, and pressure, it changes the mass-radius relationship of neutron stars considerably. The differences of the neutron star radius corresponding to maximum mass between the RMF theory and RMF* calculations are 0.23—0.33 km.

Key words neutron star, crust of neutron star, equation of state, RMF theory

The existence of neutron stars was predicted following the discovery of neutron. The radio pulsars discovered by Bell and Hewish in 1967[1] were identified as rotating neutron stars by Pacini[2]. The first theoretical calculation of neutron stars was performed by Oppenheimer and Volkoff[3], and independently by Tolman[4]. To study the neutron star, the equation of state (EOS) is crucial to determine properties of the neutron star, such as the mass range, the mass-radius relationship, the crust thickness, the cooling rate, and even the energy released in a supernova explosion. Usually, the EOS is obtained by extrapolating the theory, which is developed mainly for normal nuclear matter, to nuclear matter with extreme high isospin and high densities. Unfortunately, such extrapolation is always model dependent.

Recently, the relativistic mean field (RMF) theory has achieved great success and it has been used in describing the properties of nuclear matter, finite nuclei[5,6], rotation nuclei[6], nuclei far from β stability[7—9], and magnetic rotation[10] successfully. A number of effective interactions based on the RMF theory have also been developed, such as the nonlinear effective interactions NL1[11], NL3[12], NLSH[13], TM1[14], density-dependent effective interactions TW-99[15], DD-ME1[16], and the recently suggested PK1, PK1r, and PKDD[17]. Different from other effective interactions in RMF, the corrections for the center-of mass are taken into account in a microscopic way in PK-series and the nonlinear self-coupling for the omega and rho mesons are included. Therefore the PK-series can provide an excellent description not only for the properties of nuclear matter even at higher density but also for the nuclei in and far from the valley of beta stability[7—9]. Based on the RMF theory, lots of efforts have been devoted to get a better description for the neutron star[18—26].

Received 26 January 2005

* Supported by Major State Basic Research Development Program (G2000077407), National Natural Science Foundation of China (10025522, 10435010, 10221003) and Doctoral Program Foundation form the Ministry of Education in China

1) E-mail: mengj@pku.edu.cn

565—569

Usually in the RMF theory, the neutron star matter is treated as a kind of uniform neutron liquid together with a small concentration of protons and electrons in equal number. However, in the standard model of the neutron star[27,28], the neutron liquid region is only the interior of the neutron star. In fact, a neutron star can be roughly divided into five regions: the surface, the outer crust, the inner crust, the neutron liquid, and the core. The surface contains a negligible amount of mass. The outer crust, at densities below the neutron drip density $4\times10^{11}\ \mathrm{g\cdot cm^{-3}}$, primarily contains a coulomb lattice of nuclei and a relativistic electron gas. In the inner crust, at density above the neutron drip density, neutrons begin to leak out of nuclei. So the matter contains a lattice of neutron-rich nuclei with the free neutron gas and electron gas. Within the inner crust, higher pressure makes the nuclei merge together and form a uniform neutron liquid with a small admixture of protons and electrons. As the density continues to increase, muons and various strange particles may appear.

Using the above model for the neutron star, at density ρ below $\sim10^4\mathrm{g\cdot cm^{-3}}$, where a fraction of electrons are bound to the nuclei ^{56}Fe, Feynman, Metropolis, and Teller (FMT) derived the EOS from Thomas-Fermi method[29]. At density ρ between 10^4 and $4\times10^{11}\mathrm{g\cdot cm^{-3}}$ where free neutrons appear, the electrons are essentially free and ^{56}Fe is no longer the lowest energy state, Baym, Pethick, and Sutherland (BPS) determined the sequence of equilibrium nuclides taking into account the effect of the Coulomb lattice, and calculated the EOS in this region[30]. In the inner crust for densities between 4×10^{11} and $2\times10^{14}\mathrm{g\cdot cm^{-3}}$, where the nuclei are immersed in a sea of free neutrons which exert a pressure on the surface of the nuclei and lower the nuclear surface energy, Baym, Bethe, and Pethick (BBP) provided the corresponding EOS by describing the nuclei with a compressible liquid-drop model designed to take into accounts the effects of the free neutrons[31]. In Ref.[26], using the RMF theory with various effective interactions, the neutron star is treated as a kind of uniform neutron liquid together with a small concentration of protons and electrons in equal number. Here, in this paper, using the EOS of the neutron star from the RMF theory but replacing the EOS at low-density with those from FMT[29], BPS[30], and BBP[31] (referred as RMF* in the following), we will investigate the corresponding influences on the neutron star properties with PK1, in comparison with other effective interactions in RMF theory.

For a static global star, the Oppenheimer-Volkoff-Tolman (OVT) equation is[3,4,18]:

$$\frac{\mathrm{d}p}{\mathrm{d}r}=-\frac{[p(r)+\varepsilon(r)][M(r)+4\pi r^3p(r)]}{r[r-2M(r)]},\quad(1)$$

$$M(r)=4\pi\int_0^r\varepsilon(r)r^2\mathrm{d}r,\quad(2)$$

where $\varepsilon(r)$ and $p(r)$ are respectively the energy density and pressure for the neutron star at r. The star radius R is defined as the point at which the pressure vanishes, $p(R)=0$, and $M(R)$ is the gravitational mass. For a given EOS, the OVT equation has a unique solution which depends on a single parameter (either the baryon density, energy density or the pressure) characterizing the conditions of matter at the center. In the first theoretical work on the neutron star by Oppenheimer and Volkoff[3], by assuming that the neutron star is composed of pure noninteracting neutron Fermi gas without protons and electrons, the EOS can be easily derived as a function of the momentum k[18,32]:

$$\varepsilon(k)=\frac{1}{\pi^2}\int_0^k(k^2+m_\mathrm{n}^2)^{1/2}k^2\mathrm{d}k,\quad(3)$$

$$p(k)=\frac{1}{3\pi^2}\int_0^k(k^2+m_\mathrm{n}^2)^{-1/2}k^4\mathrm{d}k.\quad(4)$$

The EOS from RMF theory, pure neutron Fermi gas model, as well as those from FMT, BPS, and BBP model are shown in Fig.1. To show the different EOS at low density, in the insert of Fig.1, the results from the RMF theory with effective interaction PK1, pure neutron Fermi gas model, and FMT, BPS, and BBP combined calculations are respectively given as solid, dot-dashed and long dashed lines. Below the crust transition point, at which the EOS from RMF theory crosses with that from the FMT, BPS, and BBP combined calculations (i.e., the crust changes into the uniform neutron liquid), the EOS from RMF theory will be replaced by the EOS from the FMT, BPS, and BBP combined calculations. This is referred as RMF* calculation in the following. For different RMF effective interactions, the crust transition points are different. They change from $0.039\ \mathrm{fm^{-3}}$ to $0.064\ \mathrm{fm^{-3}}$. For PK1, it is $0.05\ \mathrm{fm^{-3}}$. For the given RMF effective interaction, the same crust transition point is used in the "Fermi gas + RMF" calculation.

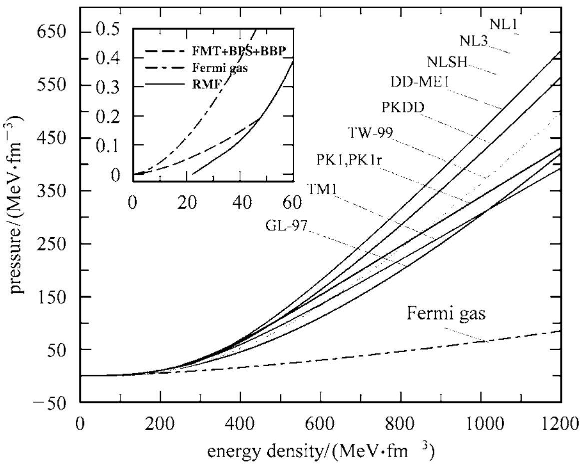

Fig.1. EOS of neutron stars by the RMF theory for effective interactions, GL-97[18], NL1[11], NL3[12], NLSH[13], TM1[14], TW-99[15], DD-ME1[16], PK1, PK1r, and PKDD[17]. The EOS at low density by FMT, BPS, and BBP model (long dashed line), pure neutron Fermi gas (dot-dashed line) and the RMF theory (solid line)[26] are given in the insert.

The mass-radius relationships for RMF theory (dot-dashed line), Fermi gas + RMF (long dashed line), and RMF* calculation (solid line) with effective interaction PK1 are shown in Fig.2, respectively. As can be seen in Fig.2, the maximum masses of the neutron stars and the corresponding radii calculated from these models are very close to each other. However, the mass-radius relationships are quite different. When the mass of the neutron star is smaller than one solar mass, the radius of the neutron star for RMF* calculation will decreases with the increase of the mass, which is in contradictory with that of the RMF result. While the Fermi gas + RMF calculation is in between, but more close to that of the RMF* calculation. It shows clearly that the EOS below the crust transition point has more influence for the low mass neutron stars than for the heavy ones.

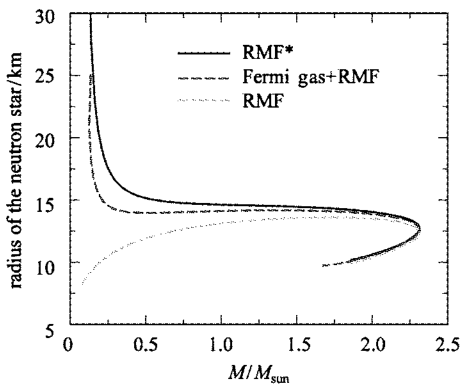

Fig.2. Mass versus radius for neutron stars by the RMF theory (dot-dashed line), Fermi gas + RMF (long dashed line), and RMF* (solid line). The effective interaction used in RMF theory is PK1.

In order to understand why the low density EOS leads to large radius difference for low-mass neutron stars but little difference for high-mass neutron stars, the pressure profiles of several representative neutron stars with central pressures, $P_c = 1.34$ MeV·fm^{-3}, 2.76 MeV·fm^{-3}, and 337.43 MeV·fm^{-3}, are shown in Fig.3. The results from RMF and RMF* calculations with effective interaction PK1 are represented by long dashed lines and solid lines respectively. At the crust transition point $p = 0.188$ MeV·fm^{-3}, the pressure profiles from RMF and RMF* calculations separate from each other. Below the crust transition point, the difference between RMF and RMF* calculations decreases with the increase of the mass of neutron star. For example, in a low-mass neutron star with central pressure $P_c = 1.34$ MeV·fm^{-3} in Fig. 3, $p(r)$ from the RMF theory quickly falls to zero at $R = 10$ km while $p(r)$ from RMF* can extend to $R \approx 20$ km. Therefore, the radius of the low-mass neutron star from RMF* is much larger than that from the RMF theory. With the increase of the mass for neutron star, $p(r)$ from RMF* calculation becomes stiffer and the thickness of the crust decreases. For the neutron star with Oppenheimer-Volkoff mass limit, $P_c = 337.43$ MeV·fm^{-3}, the radius difference between the RMF theory and RMF* is around 0.3 km. The detailed comparisons for RMF and RMF* calculations are given in the Table 1, including

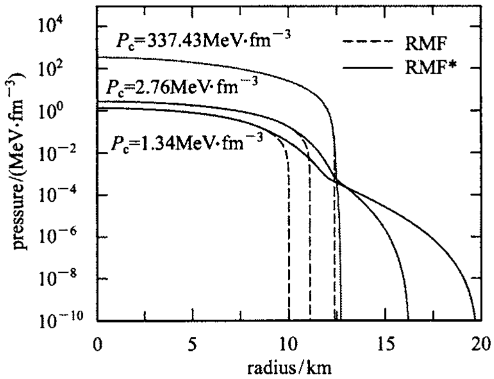

Fig.3. Pressure as a function of radius in neutron stars for different central pressures, $P_c = 1.34$ MeV·fm^{-3}, 2.76 MeV·fm^{-3}, and 337.43 MeV·fm^{-3}. With the effective interaction PK1, solid lines are the results from RMF* and long dashed lines from the RMF theory. The crust transition point is at $p = 0.188$ MeV·fm^{-3} where the results from RMF theory and RMF* deviate.

the maximum mass of OV solution, corresponding radii, central densities, energy densities, and pressures for different effective interactions. The maximum mass of OV solution, corresponding central densities, energy densities, and pressures of neutron stars for RMF theory and RMF* calculation are almost the same. However, the differences of corresponding radii are around 0.23—0.33 km.

Table 1. The maximum mass of OV solution, and their corresponding radii, densities, energy densities, and pressures at the center for neutron stars by the RMF theory[26] and RMF* for different effective interactions.

		mass limit /$M_\odot$	radius /km	density /fm^{-3}	energy density /(10^{15} g·cm^{-3})	pressure /(10^{35} dyne·cm^{-2})
DD-ME1	RMF*	2.473	12.109	0.824	1.883	8.095
	RMF	2.473	11.876	0.824	1.883	8.095
TW-99	RMF*	2.196	11.392	1.003	2.229	8.537
	RMF	2.196	11.122	1.003	2.229	8.537
TM1	RMF*	2.180	12.421	0.853	1.886	5.312
	RMF	2.180	12.088	0.853	1.886	5.312
GL-97	RMF*	2.019	10.962	1.092	2.492	8.727
	RMF	2.019	10.682	1.092	2.492	8.727
NL1	RMF*	2.809	13.404	0.658	1.530	7.146
	RMF	2.809	13.171	0.658	1.530	7.146
NL3	RMF*	2.778	13.347	0.668	1.548	7.083
	RMF	2.778	13.103	0.668	1.548	7.083
NLSH	RMF*	2.802	13.546	0.650	1.500	6.703
	RMF	2.802	13.293	0.650	1.500	6.703
PK1	RMF*	2.313	12.704	0.795	1.769	5.375
	RMF	2.313	12.388	0.795	1.769	5.375
PK1r	RMF*	2.315	12.703	0.795	1.768	5.375
	RMF	2.315	12.388	0.795	1.768	5.375
PKDD	RMF*	2.384	12.120	0.855	1.944	7.779
	RMF	2.384	11.862	0.855	1.944	7.779

In Fig.4, the mass-radius relations from the RMF* calculations with various effective interactions are shown and those from the RMF calculations[26] are given in Fig.5. There are big differences in Figs.4 and 5. Particularly for low-mass neutron star (less than one solar mass), the mass-radii behaviors for the RMF and RMF* calculations are totally different.

The masses versus the central densities of neutron star for RMF* is almost the same as in Ref. [26], i.e., both the RMF and RMF* calculations give the same mass-central density relationships. Therefore, we do not present them again here.

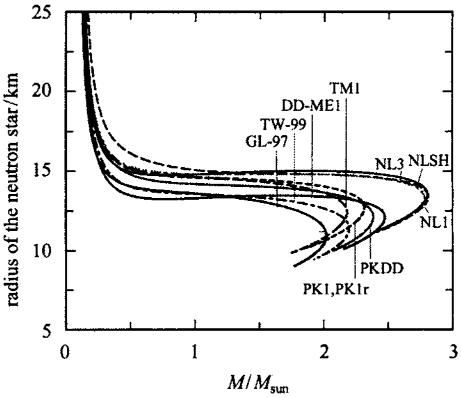

Fig.4. Masses versus radii for neutron stars for RMF* with effective interactions, GL-97[18], NL1[11], NL3[12], NLSH[13], TM1[14], TW-99[15], DD-ME1[16], PK1, PK1r, and PKDD[17].

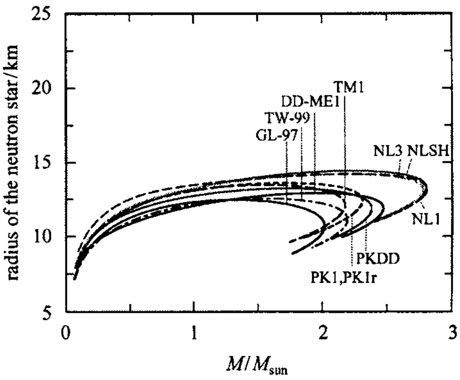

Fig.5. Same as Fig.4 but for RMF.

In summary, using the RMF theory to describe the neutron liquid region in neutron star and the Fermi gas model (Fermi gas + RMF) or FMT, BPS, and BBP model (RMF*) to describe the crust of neutron star, the properties of the neutron star are calculated and compared with those from the RMF theory. It is found that the low-density EOS has an important influence on the properties of the neutron star. Particularly totally different behaviors can be found in the mass-radius relationships in a neutron star with mass less than one solar mass. When the mass of neutron star increases, the thickness of the crust will decreases. For the OV mass neutron stars, although the low-density EOS has negligible influence on the maximum mass of OV solution, corresponding central densities, energy densities, and pressures, the differences of the neutron star radius from the RMF theory and RMF* calculations are around 0.23—0.33 km.

Zhu Zhao-Huan would like to thank the President Scholarship at Peking University for the support of this project.

References

1 Hewish A, Bell S J, Pikington J D H et al. Nature, 1968, **217**:709
2 Pacini F. Nature, 1967, **216**:567
3 Oppenheimer J R, Volkoff G M. Phys. Rev., 1939, **55**:374
4 Tolman R C. Phys. Rev., 1939, **55**:364
5 Walecka J D. Ann. Phys., 1974, **83**:491
6 Ring P. Prog. Part. Nucl. Phys., 1996, **37**:193
7 MENG J. Nucl. Phys., 1998, **A635**:3
8 MENG J, RING P. Phys. Rev. Lett., 1996, **77**:3963
9 MENG J, RING P. Phys. Rev. Lett., 1998, **80**:460; MENG J, Tanihata I, Yamaji S. Phys. Lett., 1998, **B419**:1; MENG J, Toki H, ZENG J Y et al. Phys. Rev., 2002, **C65**:041302; MENG J, ZHOU S G, Tanihata I. Phys. Lett., 2002, **B532**:209
10 Madokoro H, MENG J, Matsuzaki M et al. Phys. Rev., 2000, **C62**: 061301
11 Lee Suk-Joon, Fink J, Balantekin A B et al. Phys. Rev. Lett., 1986, **57**:2916
12 Lalazissis G A, Konig J, Ring P. Phys. Rev., 1997, **C55**:540
13 Sharma M M, Nagarajan M A, RING P. Phys. Lett., 1993, **B312**:377
14 Sugahara Y, Toki H. Nucl. Phys., 1994, **A579**:557
15 Typel S, Wolter H H. Nucl. Phys., 1999, **A656**:331
16 Nikšić T, Vretenar D, Finelli P et al. Phys. Rev., 2002, **C66**:024306
17 LONG W H, MENG J, Giai N V et al. Phys. Rev., 2004, **C69**:034319
18 Glendenning N K. Compact Stars. New York: Springer-Verlag, 1997; Glendenning N K, Schaffner-Bielich J. Phys. Rev. Lett., 1998, **81**:4564; Glendenning N K, Schaffner-Bielich J. Phys. Rev., 1999, **C60**:025803
19 Kaplan D B, Nelson A E. Phys. Lett., 1986, **B175**:57
20 Fujii H, Maruyama T, Muto T et al. Nucl. Phys., 1996, **A597**:645
21 Pons J A, Reddy S, Ellis P J et al. Phys. Rev., 2000, **C62**:035803
22 Norsen T, Reddy S. Phys. Rev., 2001, **C63**:065804; Norsen T. Phys. Rev., 2002, **C65**:045805
23 JIA H Y, SUN B X, MENG J et al. Chin. Phys. Lett., 2001, **18**:1571; JIA H Y, LÜ H F, MENG J. High Energy Phys. Nucl. Phys., 2002, **26**: 1050 (in Chinese)
(贾焕玉,吕洪凤,孟杰. 高能物理与核物理,2002,**26**:1050);
SUN B X, JIA H Y, Meng J et al. Commum. Theor. Phys., 2001, **36**: 446; JIA H Y, MENG J, ZHAO E G et al. High Energy Phys. Nucl. Phys., 2003, **27**:200 (in Chinese)
(贾焕玉,孟杰,赵恩广等. 高能物理与核物理,2003,**27**:200);
24 LI J, BAN S F, JIA H Y et al. High Energy Phys. Nucl. Phys., 2004, **28**:140—147 (in Chinese)
(李俊,班淑芳,贾焕玉等. 高能物理与核物理,2004,**28**:140—147)
25 MENG J, BAN S F, LI J et al. Phys. Atom. Nucl., 2004, **67**:1619
26 BAN S F, LI J, ZHANG S Q et al. Phys. Rev., 2004, **C69**: 045805
27 Heiselberg H, Hjorth-Jensen M. Phys. Rep., 2000, **328**:237
28 Pandharipande V R, Pines D, Smith R A. Astrophys. J., 1976, **208**:550
29 Feynman R P, Metropolis N, Teller E. Phys. Rev., 1949, **75**:1561
30 Baym G, Pethick C J, Sutherland P S. Astrophys. J., 1971, **170**:299
31 Baym G, Bethe H A, Pethick C J. Nucl. Phys., 1971, **A175**:225
32 Silbar R R, Reddy S. Am. J. Phys., 2004, **72**:892

低密度物态方程对中子星性质的影响*

朱照寰[1]　班淑芳[1]　李俊[1]　孟杰[1,2,3;1)]

1(北京大学物理学院　北京　100871)

2(中国科学院理论物理所　北京　100080)

3(兰州重离子加速器国家实验室原子核理论中心　兰州　730000)

摘要　利用相对论平均场理论描述中子星的液体区域,Fermi 气体模型或者 FMT,BPS 和 BBP 模型描述中子星外壳,分别称为 Fermi gas + RMF 和 RMF*.计算了中子星性质并且和相对论平均场理论给出的结果进行比较.虽然低密度物态方程对中子星最大质量、中心密度、能量密度和压强的影响很小,但是它对中子星的质量半径关系改变很大.对应中子星的最大质量,RMF 和 RMF*之间的半径差别为 0.23—0.33km.

关键词　中子星　中子星外壳　相对论平均场理论

2005-01-26 收稿

* 国家重点基础研究发展规划项目(G2000077407),国家自然科学基金(10025522,10435010,10221003)和教育部博士基金资助

1) E-mail: mengj@pku.edu.cn